Technical Note

Improved Homogeneity of the Transmit Field by Simultaneous Transmission with Phased Array and Volume Coil

Nikolai I. Avdievich, PhD,[1]* Sukhoon Oh, PhD,[2] Hoby P. Hetherington, PhD,[1] and Christopher M. Collins, PhD[2]

Purpose: To improve the homogeneity of transmit volume coils at high magnetic fields (≥4 T). Due to radiofrequency (RF) field/tissue interactions at high fields, 4 T to 8 T, the transmit profile from head-sized volume coils shows a distinctive pattern with relatively strong RF magnetic field B_1 in the center of the brain.

Materials and Methods: In contrast to conventional volume coils at high field strengths, surface coil phased arrays can provide increased RF field strength peripherally. In theory, simultaneous transmission from these two devices could produce a more homogeneous transmission field. To minimize interactions between the phased array and the volume coil, counter rotating current (CRC) surface coils consisting of two parallel rings carrying opposite currents were used for the phased array.

Results: Numerical simulations and experimental data demonstrate that substantial improvements in transmit field homogeneity can be obtained.

Conclusion: We have demonstrated the feasibility of using simultaneous transmission with human head-sized volume coils and CRC phased arrays to improve homogeneity of the transmit RF B_1 field for high-field MRI systems.

Key Words: TEM; high field MRI; CRC surface coil; RF field inhomogeneity; phased array
J. Magn. Reson. Imaging 2010;32:476–481.

AT HIGH MAGNETIC FIELDS (≥4 T) radiofrequency (RF) field/tissue interactions substantially alter the RF field homogeneity over the human head when conventional volume coils are used (1–3). Although the reception profile of the coil, B_1^-, can often be compensated for adequately in post-processing (4), residual inhomogeneity in the transmission field, B_1^+, reduces the accuracy of measurement when B_1 compensating pulses are not used (5–8). Hereafter, B_1^+ and B_1^- are the circularly polarized RF magnetic fields rotating with and opposite nuclear precession, respectively (9,10). Due to RF field/tissue interactions at high field the transmit and receive RF magnetic field profiles produced by head-sized volume coils show a distinctive pattern of inhomogeneity, with relatively high sensitivity in the center of the human brain (1,2). For example, SNR measured in the center of the central transaxial slice of the head was higher than that in the periphery by 30% at 4 T (1) and by 75% at 7 T (2). Previously, B_1^+ field inhomogeneity corrections at high magnetic fields have been demonstrated experimentally (11–13) and numerically (3,14,15) by using phased arrays (12,13,15,16) or multi-port driven volume coils (3,11). These methods can improve transmit RF field homogeneity by combining the most homogeneous mode with higher order modes possessing much higher peripheral sensitivity (8,9,17). Since these modes are intrinsically characterized by a substantial level of nonuniformity in phase, linear combination of the fields can result in substantial destructive interference. Alternatively, B_1^+ field inhomogeneity can be compensated by using simultaneous transmission with a volume coil and a surface coil phased array. Since phased arrays provide substantially higher peripheral sensitivity than a volume coil, simultaneous transmission from the array can enhance the peripheral RF magnetic field improving overall homogeneity. When the array is driven such that the total phase shift over the entire circumference of the array is 2π, ideally a circularly polarized RF magnetic field B_1^+ is generated which is similar to that of a volume coil. Importantly, the phase distributions of the RF magnetic fields generated by the volume coil and the array are similar, allowing them to be recombined constructively. In theory, simultaneous transmission from these two devices can provide an RF

[1]Department of Neurosurgery, Yale University, New Haven, CT, USA.
[2]Center for NMR Research, Department of Radiology, Pennsylvania State University College of Medicine, Hershey, PA, USA.
Contract grant sponsor: National Institutes of Health (NIH); Contract grant numbers: M01-RR12248, R01-EB00473, R01-EB009871, R01-EB000454.
*Address reprint requests to: N.I.A., Ph.D., Department of Neurosurgery, Yale University, MRRC/TAC, 300 Cedar Str, New Haven, CT 06519. E-mail: nikolai.avdievich@yale.edu
Received October 9, 2009; Accepted April 29, 2010.
DOI 10.1002/jmri.22257
Published online in Wiley InterScience (www.interscience.wiley.com).

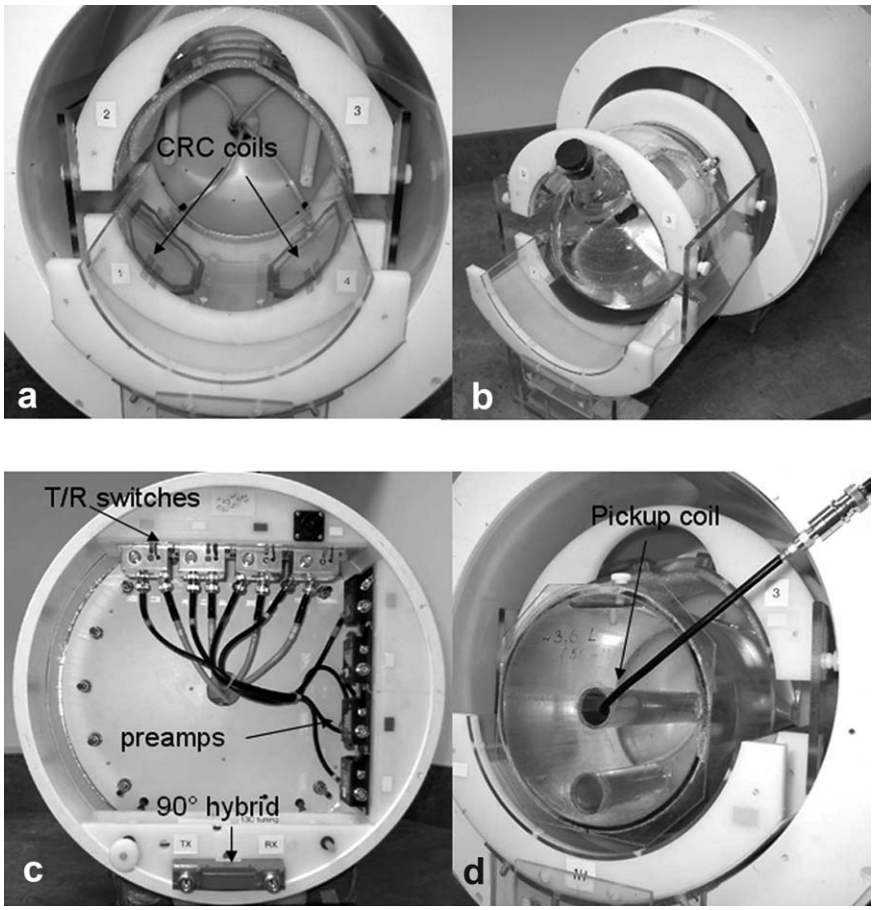

Figure 1. Photographs of the front side of the TEM volume coil (**a**) with the CRC phased array placed inside of the TEM and (**b**) with the array moved out of the volume coil. **c:** Back view of the TEM/CRC phased array assembly with all the T/R switches and preamplifier mounted on the volume coil's shell. **d:** TEM/CRC array assembly with the cylindrical phantom placed inside of the array. A 1-cm pickup coil was used for phase adjustment as described in the text.

field which is more homogeneous. In practice, however, the strong coupling between most conventional phased arrays and the volume coils prevents their simultaneous operation. To avoid interactions between the volume coil and phased array, counter rotating current (CRC) surface coils, each consisting of two parallel rings carrying opposite currents can be used in the phased array (18,19). Simultaneous reception for improved sensitivity in the center of the human brain has also been reported using a volume coil and a CRC phased array (20).

This work describes the use of a phased array of CRC coils in conjunction with a head-sized transverse electromagnetic (TEM) volume coil for simultaneous transmission at 4 T. Specifically we have: 1) experimentally compared transmit performance of the TEM volume coil/CRC array combination to that of the TEM alone on a human head and a phantom; 2) theoretically verified the experimental results using finite difference time domain (FDTD) method; 3) calculated changes in local and average specific absorption rate (SAR) when TEM/CRC array used simultaneously as compared to TEM alone; and 4) performed a numerical evaluation of the improvements in homogeneity possible with combining a TEM coil and an 8-element CRC array with control of current magnitude and phase in individual elements. Description of the method and some preliminary results of this work have been reported previously (20,21).

MATERIALS AND METHODS

Coil Design and Construction

A 16-element quadrature TEM head-sized volume coil (element inner diameter = 31.8 cm, shield diameter = 38 cm, length = 23.9 cm) was constructed for 4 T as described previously (1,2,22). No active detuning was incorporated into the volume coil. The CRC phased array circumscribing the head consisted of four 9 × 10 cm CRC surface coils (Fig. 1a) constructed using 6.4 mm copper tape. Each CRC coil consisted of two coplanar octagonal loops separated by 9 mm and connected in series. The coils were placed on an acrylic holder with 20.3 cm outer diameter (wall thickness 3.2 mm) at about 45° in respect to horizontal and vertical axes. To provide a better fit, the coil holder was split into two portions with the position of the top portion being vertically adjustable (Fig. 1a and b). The intrinsic decoupling between surface coils loaded with a head or a phantom was better than −20 dB. Preamplifier decoupling (23) was used to improve the sensitivity profile of the volume coil during reception (20). Preamplifiers (input impedance ~5 Ohm) were purchased from Advanced Receiver Research (Burlington, CT, USA) and modified as described by Beck and Blackband (24). The preamplifiers were mounted at the volume coil shell and were protected during the transmission by home-built T/R switches providing better than −45 dB isolation and about −0.15 dB

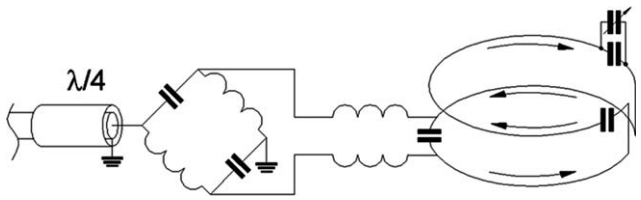

Figure 2. Schematic of the individual CRC coil including matching network. CRC coil is shown schematically as two circular loops (see text for details of the CRC coil geometry).

insertion loss (Fig. 1c). The intrinsic isolation between the volume and CRC coils was better than −15 dB. Each CRC coil had variable tuning incorporated into the coil and was matched as shown in Fig. 2. Tri-axial baluns were used for each channel to prevent shield currents.

The interface connecting RF to the TEM/CRC array combination consisted of a four-way splitter and four T/R switches (Fig. 3). The interface provides delivery of RF power to the array during transmission and connection of the surface coils to the preamplifiers during reception. This enables both simultaneous transmission and reception with the CRC array and the TEM volume coil. During transmission, the RF power was distributed between the TEM and the phased array using a two-way splitter (or a directional coupler). When necessary a variable attenuator provided further attenuation of the transmit power. The four-way splitter was constructed from connectorless 90° hybrids (Anaren Microwave, NY, USA). The phases of RF were adjusted so as to provide 0°, 90°, 180°, and 270° phase shifts at the corresponding coils in the array. To ensure that the B_1 fields generated by the array and the TEM coil add constructively in the center of a head (or a phantom), we adjusted the phase shift between the TEM and the CRC array. For that purpose we used a cylindrical phantom (3.6 L, 50 mM NaCl) with a 2-cm hole in its center and a small (1 cm diameter) pickup coil. The pickup coil was placed inside of the phantom near the center of the coils as shown in Fig. 1d.

Data Collection

Data were collected using a 4 Tesla Varian Inova system (Varian Associates, Inc., Palo Alto, CA, USA). To test the coil performance, B_1^+ maps (multiple slices) were collected using a rapid interleaved gradient echo approach (25) with 64 × 64 resolution, TR = 1 second, 5/5 mm slice thickness/gap centered on the matched gradient echo images. To determine the B_1 amplitude produced by the coils, two nominal 60° excitation pulses were applied sequentially prior to incrementing the phase encoding value. After correcting for slice profile, the ratio of the amplitudes of the image acquired with data following the second pulse to that of the image acquired with data following the first pulse is given by cos (θ), where θ is an RF pulse angle. All the B_1^+ maps are presented below as distributions of the pulse angle.

Numerical Simulations

A numerical model of a human head inside a CRC array and a TEM coil much like those used in experiment was created for use with the FDTD method for calculating electromagnetic fields. The model had a resolution of 5 mm. Three field calculations were performed, driving the four-element array and the volume coil separately to determine B_1^+ phase distribution and relative power dissipation produced by each, and then simultaneously to determine the final field and SAR distribution when phases and magnitudes like those in experiment were used. In each calculation, multiple current sources were used to excite the coils with the expected current distribution at 170 MHz. As in the experiment, the CRC coils were driven with equal magnitude and fixed phase relative to each other, with phase being proportional to the angle describing the position of each coil about a central axis. When driven simultaneously the ratio of power delivered to the volume coil to that in the array was 2:1 with the relative phase between the TEM and array of CRC coils designed to produce maximum field strength at the center of the head model, as in the experiment. Evaluations of 10-g average SAR (SAR_{10g}), head-average SAR (SAR_{ave}), and efficiency (magnitude of B_1^+ per watt of input power) was performed for the TEM alone and for the TEM combined with the CRC.

To explore possibilities for the future, an additional set of simulations was performed with eight CRC elements having roughly equal spacing about the head. A simple gradient descent optimization routine was used to maximize the field homogeneity in this arrangement, with a total of 18 independent variables including magnitude and phase of the current in each of the eight CRC coils and in the TEM. Briefly, from a given set of magnitudes and phases, variations in the magnitude and phase of each channel were routinely explored. Any time a variation which improved the homogeneity was discovered, it was adopted as the new starting point. This process was repeated until no

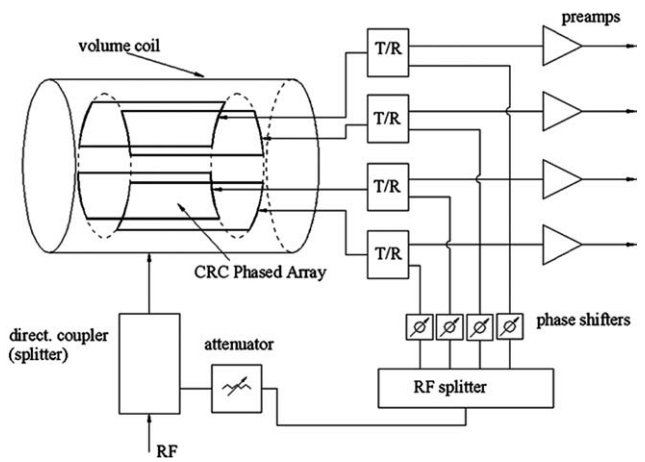

Figure 3. Schematic of the experimental setup for simultaneous transmission and reception with the CRC phased array and the volume coil.

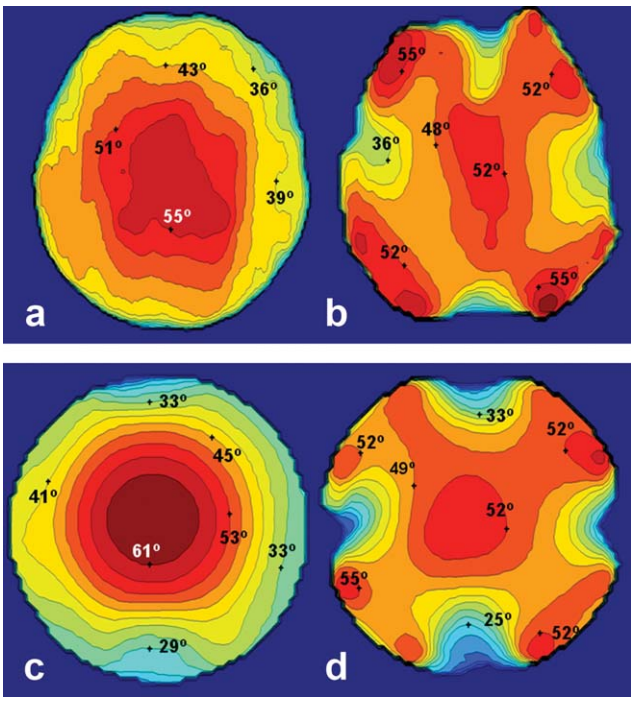

Figure 4. Top: B_1^+ maps obtained on a human head using (**a**) TEM volume coil alone and (**b**) during the TEM/CRC array simultaneous transmission. Bottom: B_1^+ maps obtained on a 3.0 L spherical phantom using (**c**) TEM volume coil alone and (**d**) during the TEM/CRC array simultaneous transmission.

further improvements could be found. Although this method by itself does not guarantee a global optimum, starting with different initial magnitude and phase configurations and allowing very large maximum variations in magnitude and phase produced very similar results.

All field calculations were performed using commercially-available FDTD software (xFDTD, Remcom Inc., State College, PA, USA), with post-processing (including phase adjustment between array and TEM for the four-element array case and 18-variable optimization in 8-element array case) performed in Matlab (The Mathworks).

RESULTS

Figure 4a and b show experimental B_1^+ maps in a human head obtained by the TEM volume coil alone (Fig. 4a) and during simultaneous transmission from the volume coil and the four-element CRC phased array (Fig. 4b). A 2:1 ratio of transmit RF power between the volume coil and the array was used in this experiment. The same RF power was used for both B_1^+ maps. Our method can also be utilized at higher magnetic field strengths where B_1 inhomogeneity becomes more severe (2). To further increase center-to-periphery ratio of the B_1 field and, thus, mimic conditions seen in 7 T human head images, where the B_1 varies by more than a factor of 2 (2), a large 3.0 L spherical phantom (outer diameter 21.5 cm) filled with 50 mM NaCl (conductivity – 0.65 S/m) was used. To compensate for the greater decrease in peripheral B_1 the RF power was split in 1:1 ratio between the TEM and the phased array. Figure 4c and d demonstrate results of the experiment for the TEM alone (Fig. 4c) and the combined TEM/CRC array (Fig. 4d).

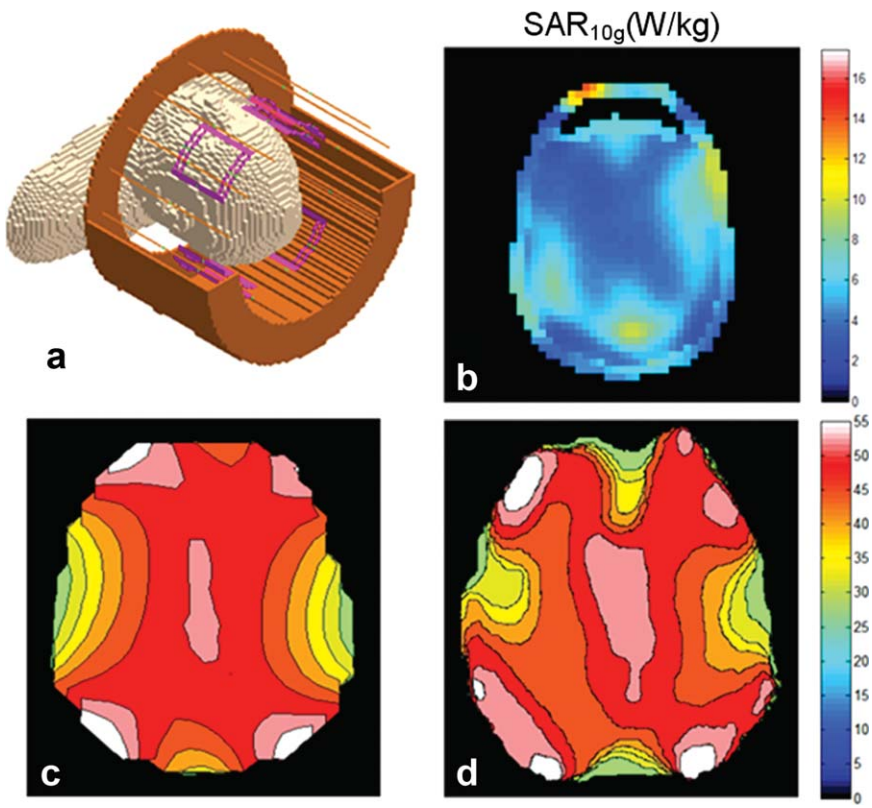

Figure 5. Simulation results for the TEM/four-channel CRC phased array combination. **a:** Coil/head geometry used in simulations. CRC surface coils are shown in purple. Shield of the TEM coil is partially cut away for better visualization. **b:** Distribution of SAR_{10g} on the axial slice through the head containing location of maximal SAR_{10g} while array is driven to induce an SAR_{ave} of 3.2 W/kg. SAR levels in actual sequence would also depend on number, shape, duration, and amplitude of pulses as well as TR (26). **c:** Simulated and (**d**) experimental B_1^+ (flip angle) distributions on the axial slice through the center of the brain with identical color maps to facilitate comparison.

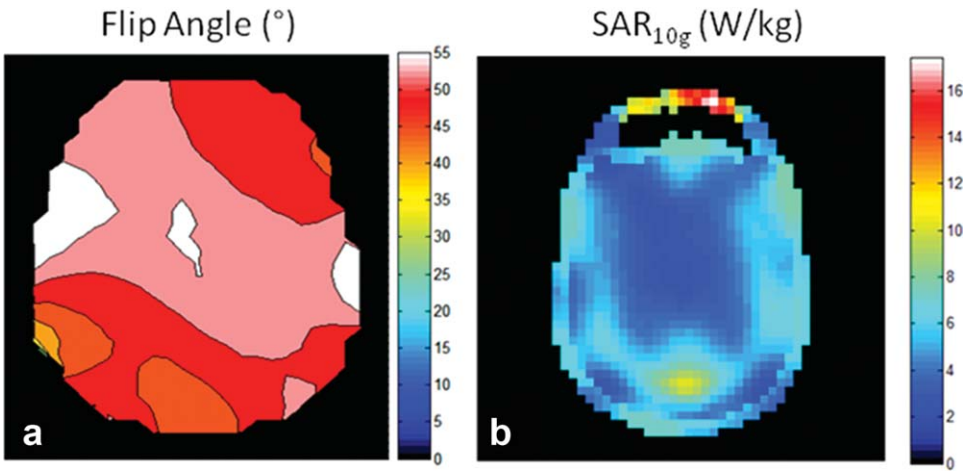

Figure 6. Optimum achievable B_1^+ (flip angle) map on an axial slice through the center of the brain (**a**) and corresponding SAR_{10g} distribution on the axial slice through the head containing the maximal SAR_{10g} (**b**) for simulated TEM/CRC array with eight CRC elements each having controllable current magnitude and phase. SAR_{10g} distribution is presented for an SAR_{ave} of 3.2 W/kg.

Figure 5 shows the B_1^+ map (pulse angle distribution) and the corresponding distribution of SAR_{10g} calculated from the numerical simulations on an axial plane through the center of the brain for the TEM/four-element CRC array combination. For comparison, Fig. 5d shows experimentally-measured B_1^+ distribution (as in Fig. 4b) using the same color scale.

Figure 6a shows the numerically simulated axial B_1^+ map optimized for the maximum RF field homogeneity obtained with the TEM volume coil and the CRC phased array consisting of eight elements, each with controllable current magnitude and phase. Figure 6b depicts corresponding distribution of SAR_{10g}. The B_1 homogeneity estimated from simulated B_1^+ maps as a standard deviation (SD), while averaging over the entire head, measured 12.1% and 5.6% of the mean B_1^+ value for the TEM volume coil alone and TEM/eight-element CRC array combination, respectively. For comparison, measured in the same way (SD over entire head) homogeneity of the TEM/four-element CRC array combination (Fig. 5) was very similar to that of the TEM coil alone mostly due to stronger inhomogeneity in the areas not covered by the CRC surface coils.

Table 1 presents the numerical values for SAR_{ave} and SAR_{10g} obtained for the TEM resonator alone, the TEM with the four-element CRC array when simulated as driven in the experiment, and the TEM with the eight-element CRC array when optimized for maximum RF field homogeneity. In each case, the SAR values given correspond to an average B_1^+ field of 3 μT in the axial slice through the center of the brain.

DISCUSSION

In human MRI at field strengths up to 3T, a volume coil for transmission with a phased array for reception is standard. The potential to use the array and volume coil simultaneously during transmission could have major implications for improving control of the RF excitation field. As seen in Fig. 4a and b, the transmit B_1 field obtained during simultaneous transmission on a human head is significantly more homogeneous than that obtained by the volume coil alone in the regions covered by the array. Similarly, the transmit B_1 field obtained using the TEM and the CRC array simultaneously on a large phantom (Fig. 4d) was more homogeneous than that obtained by the TEM coil alone (Fig. 4c). Notably, the power required to achieve an average pulse angle of 90° across an entire axial slice was the same for both configurations within 1 dB.

There is good agreement between the simulated and the experimental RF pulse angle distributions (B_1^+ map) obtained for a human head using TEM/four-channel CRC array combination (Fig. 5). Increasing the number of CRC coils would reduce the effects of the residual low B_1 regions seen between the coils, as shown in Fig. 6. The B_1 homogeneity estimated from simulated B_1^+ maps as a standard deviation, while averaging over the entire head, measured 12.1% and 5.6% for the TEM volume coil alone and TEM/eight-channel CRC array combination, respectively. Previously, high field inhomogeneity corrections have been demonstrated by using phased arrays (12,13,15,16) or multi-port driven volume coils (3,11). In these methods, the homogeneous mode and higher order

Table 1
SAR_{ave}, Location and Values of Maximum SAR_{10g} During Production of a 3.0 μT Average B_1^+ Field for Different Transmit Coil Configurations

Coil configuration	SAR_{ave} (W/kg)	Max. SAR_{10g} (W/kg)	Location of maximum SAR_{10g}
TEM Only	2.94	9.81	Right masticator space at level of zygomatic arch
TEM with 4-element CRC array	1.83	7.96	Scalp anterior to frontal sinus
TEM with 8-element CRC array	1.42	7.75	Scalp anterior to frontal sinus

modes are driven simultaneously to increase B_1 near the surface and improve the overall homogeneity. However, the different phase distributions of the modes results in spatially varying phase cancellation across the volume, decreasing the overall efficiency of transmission. Conversely, although the TEM and phased array have different spatial profiles their phase distributions are similar enabling efficient combination.

As seen in Table 1, both SAR_{ave} and SAR_{10g} are lower for the TEM/CRC array than for the TEM alone for a given average B_1 value in the brain. This also could be further improved when a CRC array with a greater number of elements is used. This may be because the CRC array, having a shorter total length and tighter fit, is more efficient than the TEM coil. Due to the greater homogeneity and lower SAR of the combined array, the CRC array should be preferable for most cases when imaging the brain.

CONCLUSIONS

We have developed a four-channel CRC phased array capable of simultaneous transmission and reception together with a TEM volume head coil. Using this configuration facilitates significant improvements in the homogeneity of the transmit B_1 profile in human brain with reduction of SAR as compared to the volume coil alone. Further improvements in B_1 field homogeneity can be obtained with larger numbers of surface coils in the phased array.

REFERENCES

1. Vaughan JT, Hetherington HP, Otu JO, Pan JW, Pohost GM. High frequency volume coils for clinical NMR imaging and spectroscopy. Magn Reson Med 1994;32:206–218.
2. Vaughan JT, Garwood M, Collins CM, et al. 7T vs. 4T: RF power, homogeneity, and signal-to-noise comparison in head images. Magn Reson Med 2001;46:24–30.
3. Ibrahim TS, Robert Lee, Baertlein BA, Abduljalil AM, Zhu H, Robitaille P-ML. Effect of RF coil excitation on field inhomogeneity at ultra high fields: a field optimized TEM resonator. Magn Reson Imaging 2001;19:1339–1347.
4. Belaroussi B, Milles J, Carme S, Zhu YM, Benoit-Cattin H. Intensity non-uniformity correction in MRI: Existing methods and their validation. Med Image Anal 2006;10:234–246.
5. Tannus A, Garwood M. Adiabatic pulses. NMR Biomed 1997;10: 423–434.
6. Katscher U, Börnert P, Leussler C, van den Brink JS. Transmit SENSE. Magn Reson Med 2003;49:144–150.
7. Zhu Y. Parallel excitation with an array of transmit coils. Magn Reson Med 2004;51:775–784.
8. Ledden, PJ, Cheng, Y. Improved excitation homogeneity at high frequencies with RF pulses of time varying special characteristics. In: Proceedings of the 12th Annual Meeting of ISMRM, Kyoto, Japan, 2004 (Abstract 38).
9. Hoult DI. The principle of reciprocity in signal strength calculations - a mathematical guide. Concepts Magn Reson 2000;12(4): 173–187.
10. Collins CM, Yang QX, Wang JH, et al. Different excitation and reception distributions with a single-loop transmit-receive surface coil near a head-sized spherical phantom at 300 MHz. Magn Reson Med 2002;47:1026–1028.
11. Seifert F, Rinnenberg H. Adaptive coil control: SNR optimization of a TR volume coil for single voxel MRS at 3T. In: Proceedings of the 10th Annual Meeting of ISMRM, Honolulu, Hawaii, 2002 (Abstract 162).
12. Adriany G, Van de Moortele P-F, Ritter J, et al. A geometrically adjustable 16-channel transmit/receive transmission line array for improved RF efficiency and parallel imaging performance at 7 Tesla, Magn Reson Med 2008;59:590–597.
13. Avdievich NI, Pan JW, JM Baehring, DD Spencer, Hetherington HP. Short Echo Spectroscopic Imaging of the Human Brain at 7T Using Transceiver Arrays. Magn Res Med 2009;62:17–25.
14. Hoult DI. Sensitivity and power deposition in a high-field imaging experiment. J Magn Reson Imaging 2000;12:46–67.
15. Collins CM, Liu W, Swift BJ, Smith MB. Combination of optimized transmit arrays and some receive array reconstruction methods can yield homogeneous images at very high frequencies. Magn Reson Med 2005;54:1327–1332.
16. Plaska J, Leussler C. Hybrid TEM/loop coil array for parallel high field MRI. In: Proceedings of the 16th Annual Meeting of ISMRM, Toronto, Canada, 2008 (abstract 149).
17. King SB. Eigenmode analysis for understanding phased array coils and their limits. Conc Magn Reson B 2006;29B:42–49.
18. Froncisz W, Jesmanowicz A, Kneeland JB, Hyde JS. Counter rotating current local coils for high-resolution magnetic resonance imaging. Magn Reson Med 1986;3:590–603.
19. Hyde JS, Froncisz W, Jesmanowicz A, Kneeland JB. Simultaneous image acquisition from the head (or body) coil and a surface coil. Magn Reson Med 1988;6:235–239.
20. Avdievich NI, Hetherington HP. High-field head RF volume coils using transverse electromagnetic (TEM) and phased array technologies. NMR in Biomed 2009;22:960–974.
21. Avdievich, NI, Hetherington, HP. Improved homogeneity of the transmit field due to simultaneous transmission with phased arrays and volume coils. In: Proceedings of the 14th Annual Meeting of ISMRM, Seattle, Washington, 2006 (Abstract 2567).
22. Avdievich NI, Hetherington HP. A 4T Actively detuneable transmit/receive ^{1}H transverse electromagnetic (TEM) and 4-channel receive-only phased array for ^{1}H human brain studies. Magn Reson Med 2004;52:1459–1464.
23. Roemer PB, Edelstein WA, Hayes CE, Souza SP, Mueller OM. The NMR phased array. Magn Reson Med 1990;16:192–225.
24. Beck BL, Blackband SJ. Phased array imaging on a 4.7 T/33 cm animal research system. Rev Sci Instrum 2001;11:4292–4294.
25. Pan JW, Twieg DB, Hetherington HP. Quantitative spectroscopic imaging of the human brain. Magn Reson Med 1998;40:363–369.
26. Collins CM, Li S, Smith MB. SAR and B1 field distributions in a heterogeneous human head model within a birdcage coil. Magn Reson Med 1998;40:847–856.